Contact angles of liquid metals on quasicrystals

Contact angles of liquid metals on quasicrystals

Claire Bergman[1,2]**, Christophe Girardeaux**[1,2]**,
Carine Perrin-Pellegrino**[1,2]**, Patrick Gas**[1,2]**,
Jean-Marie Dubois**[3] **and Nicolas Rivier**[4]

[1] Aix-Marseille Université, IM2NP, Faculté des Sciences et Techniques, Campus de
Saint-Jérôme F-13397, Marseille cedex 20, France

[2] CNRS, IM2NP (UMR 6242), Faculté des Sciences et Techniques, Campus de Saint-Jérôme
F-13397, Marseille cedex 20, France

[3] Institut Jean Lamour (FR 2797 CNRS-INPL-UHP), Ecole des Mines, Parc de Saurupt,
F-54042 Nancy Cedex, France

[4] IPCMS, Université Louis Pasteur, F-67084 Strasbourg Cedex, France

E-mail: claire.bergman@l2mp.fr

Abstract
Wetting with μm-sized Pb droplets on thin polycrystalline films of decagonal $Al_{13}Co_4$ is
reported. The films were prepared under high vacuum conditions in order to have Pb droplets
lying on a clean surface. The method used is sequential deposition and annealing of specific
stackings of Al and Co layers of nanometric thicknesses. A 300 nm thick Pb slab was then
deposited on top of the films and dewetting experiments were followed *in situ* in a scanning
Auger microprobe. The contact angle between the Pb droplet and the surface of the film is
measured to be $49° \pm 7°$. Further investigation performed by cross section transmission electron
microscopy allows us to better characterize the interface. Taking into account the rugosity of the
film, it is concluded that there is partial wetting of the film, which corresponds to a smaller
contact angle. The comparison with other results obtained either with pure metals or with a
cubic AlCo compound leads to the conclusion that the wetting behaviour of Pb on the surface of
a decagonal compound is close to that of a metal with a high melting point and not significantly
different from that of a crystalline compound with a small unit cell.

1. Introduction

For more than two decades, the specific properties of
quasicrystals have attracted attention in different fields
from solid-state physics and crystallography to material
science. Quasicrystals (QCs) are metallic alloys which
show a quasiperiodic translational order and an orientational
order associated with the classically forbidden symmetry
axes [1]. A central question was to determine whether
quasiperiodicity leads to physical properties different from
those of corresponding crystalline compounds. The first
QC was prepared by Shechtman in 1982 but the results
were published two years later [2]. Afterwards, intensive
investigations led to the possibility to grow single-grain
samples with sizes up to a few centimetres large [3], mainly
based on aluminium and hence to measure physical properties.

It turns out that the QC's rich in aluminium for example
have a particularly low electrical conductivity which decreases
with temperature, contrary to the behaviour of 'normal'
metals [4, 5]. Their thermal conductivity is surprisingly low
since at room temperature the values of the quasicrystalline i-
AlCuFe and i-AlPdMn compounds are more than two orders
of magnitude lower than that of aluminium metal. As other
intermetallic compounds they are very brittle in bulk form [6].
This is the reason why, in case of technological applications,
they will be employed as surface coatings or as composites and
not as bulk materials.

Since 1991, unusual surface properties have been
reported [7], including low friction coefficients, high contact
angles with water and good resistance to oxidation [8, 9].
More recently it was shown [10, 11] that in the case of
i-AlCuFe annealed under low oxygen pressure, the surface

energy remains low up to 673 K as long as the layer of alumina remains amorphous and limited to a few atomic layers. Because these anomalous surface properties were investigated in air, an environment where aluminium-rich materials are covered with an aluminium oxide layer, it may be debated whether the observed surface properties are due to the oxide layer, or specific to the quasicrystalline structure. Indeed, the low electrical and thermal conductivities of quasicrystals as mentioned above are due to their specific electronic structure which shows a strong reduction of the electronic density of states at the Fermi level [12]. This characteristic has been evoked to explain the low surface energy observed in previous measurements. The first studies of clean surfaces of quasicrystals were published in the early 1990s (for a review see [13]). They were focusing on the atomic and electronic structures of the surface. In order to get rid of the oxide layer, several methods have been proposed (cleavage, sputtering, annealing, etc) [14].

In a previous work [15], in order to investigate the effect of the structure on the wetting properties, a comparative study of the wetting of Pb on the surface of thin polycrystalline films of two compounds in the Al/Co system—one with a cubic (CsCl type) crystalline and the other with a decagonal quasicrystalline structure—has been performed. From this study, we deduced that the contact angles observed on both Al–Co compounds were slightly influenced by the crystalline structure.

The present paper focuses on experiments carried out on the decagonal phase d-Al$_{13}$Co$_4$ in reporting a careful characterization of the interface from the micrometre to the nanometre scale. Moreover, these results are discussed in the frame of the results observed in the growth of films of different metallic elements on quasicrystalline substrates. In this study, special care was taken to prevent the formation of an aluminium oxide layer on the surface of the compound before and during the wetting experiment. Let us recall that this method has allowed, for the first time, the study in clean conditions of the wetting of a liquid metal on quasicrystalline surfaces [15].

Recently, several studies on the study of the growth of thin films of metals on a quasicrystalline surface have been published in the literature. In the next section we will review briefly some of these results and explain why the equilibrium conditions may differ from those of our experiments.

2. Growth of metallic thin films on a quasicrystalline surface

It has been recognized for several decades that vapour-deposited thin films can grow by a number of distinct modes. Bauer [16, 17] proposed a topological classification in which the three principal modes were named after their original investigators: Frank and van der Merwe [18] (monolayer-by-monolayer, or FM growth), Stranski and Krastanov [19] (layer growth up to one or a few monolayers followed by 3D crystallite growth, SK growth); Volmer and Weber [20] (formation of 3D crystallites without a preceding adsorbed layer, VW growth).

An explanation of the different growth modes can be formulated in terms of surface energy criteria [16]. If the condensate (adsorbate) has a surface energy γ_A, the substrate γ_S and the interface between the two γ_{AS}, then the condition $\gamma_A + \gamma_{AS} < \gamma_S$ will favour the covering over the substrate by spreading of the condensate (wetting or FM mode) while $\gamma_A + \gamma_{AS} > \gamma_S$ will favour non-wetting (SK or VW mode). The prediction of the type of growth modes from energetic considerations is in fact a complex problem which depends on the epitaxial relations between the two crystal lattices (misfit) and the degree of strain.

It is worth noting that thin film growth modes are temperature-dependent and that the validity of the classification outlined above depends on achieving local surface equilibrium; surface diffusion processes must be rapid in comparison with the rate of vapour impingement and with the timescale of observations. When the deposited material is prepared at relatively low temperature (i.e. low mobility of the atoms) or when the vapour flux is relatively high, metastable growth topographies may form that are not at equilibrium due to slow kinetics. When the melting point of the deposited material (film) is lower than that of the substrate, one way to bring the system back to equilibrium is to heat the system up to the melting point of the film: at this temperature, the film can adopt an equilibrium form.

This is what we have done in our experiments: (i) growth of a Pb film of a few nanometres (a nanocrystalline film that we called previously a metastable growth topography) on the substrate, (ii) annealing of the specimen up to the melting point of Pb. There is dewetting of the initial continuous film and formation of droplets of lead (the deposited film takes an equilibrium form).

In the case of the growth of thin films on a quasicrystalline surface, numerous studies have shown very interesting results concerning the behaviour of the crystalline/quasicrystalline interface. A survey of the literature reveals that different situations are observed; for example, in the case of noble metals [21], deposition of Au and Pt (with some pre-deposited In) on the surface of d-AlNiCo quasicrystal, yielded an epitaxial layer whereas a deposition of Ag did not. Another investigation of Ag film growth reported on i-AlPdMn surface shows that at high coverage (>10 ML), islands start growing normally to form ultimately hexagonal nanocrystals [22]. Fe deposition on i-AlPdMn indicates that the layers are disordered and that there is no intermixing [23]. The deposition of semiconducting species such as Si has been investigated on the ten-fold surface of d-AlNiCo leading to the conclusion that at coverage above one monolayer, the Si overlayer follows a rough 3D growth mode [24] (for a more recent review see [25]).

These results constitute a different approach from ours but it is of great interest to bring the resulting conclusions together.

3. Preparation of quasicrystalline thin films

Solid-state reaction allows the formation of intermetallic compounds without the need for high-temperature processing and with relatively good control of the growth kinetics

and layer morphology. This process often called reactive diffusion [26] is characterized by a competition between stable and metastable phases linked to the conditions of the phase nucleation under constraints [27]. Thus it can lead to the formation of thermodynamically stable phases but also of metastable ones when the reaction occurs between very thin and/or multilayer films [28]. It is a very suitable method to elaborate thin films of materials with limited range of stability such as binary quasicrystals. The Al–Co phase diagram is very complex in the Al-rich region: indeed, four stable compounds and several metastable structures have been observed in bulk material between Al_5Co_2 and Al_9Co_2 [29]. For some of these compounds, an annealing time of 1580 h at 1273 K was necessary to reach equilibrium, revealing that kinetics could play a significant role in the formation of the phases in that range of compositions. First discovered by Ma and Kuo, the decagonal phase in Al–Co system was observed within a very limited range of stability [30, 31]. Further studies on the phase diagram [32, 33] lead to the conclusions that the d-phase was metastable. But a 'metastable' phase is different from an 'unstable' phase which could be not suitable for investigation; in a previous work [34] the thermal stability of the decagonal thin film obtained by reactive diffusion was investigated through further annealing treatments up to 1073 K. In this same study [34], we have shown from electron diffraction and x-ray diffraction measurements that a stack of Al/Co bilayers of nanometric thickness forms, upon annealing at about 700 K, a single-phase decagonal quasicrystalline film with homogeneous microstructure.

4. Experimental details

The multilayers were made by successive electron-beam evaporations of high-purity Al(99.9999 at.%) and Co(99.9999 at.%) on an oxidized Si substrate at room temperature. The base pressure during the evaporation was in the 10^{-4}–10^{-5} Pa range for both metals. The Al and Co layer thicknesses were monitored during evaporation with a quartz balance. The nominal [Al]/[Co] atomic ratio of the sample corresponds to 13/4. The total thickness of multilayer samples was equal to 300 nm and the number of Al/Co units equal to 5, that corresponds to a period of 60 nm. The transformation into the d-phase was achieved by an appropriate annealing treatment [34].

A suitable method for studying the wetting of oxidizable surfaces is the dewetting of thin ($\sim$100 nm) slabs, in our case Pb slab [35]. First, the films of d-$Al_{13}Co_4$ compounds are prepared (as explained above [34]) in an ultrahigh vacuum deposition chamber. Then, in the same apparatus and without breaking the vacuum, the lead slab is deposited on the substrates. This constitutes the original feature of the process. In addition, the Pb layer protects the quasicrystalline surface when the samples are transferred to the scanning Auger microprobe (SAM).

After preparation, the Pb/d-$Al_{13}Co_4$ sample deposited on an oxidized silicon wafer, was transferred in air, from the deposition chamber to a CAMECA Nanoscan 100 SAM, equipped with a STAIB Instruments analyzer, a 6 keV CAMECA Duoplasmatron ion gun, and a home-built heating
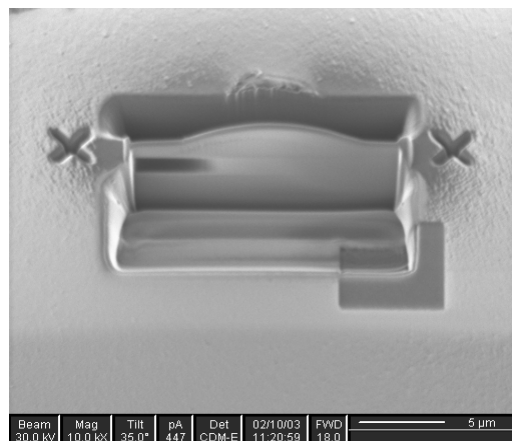

Figure 1. Focused ion beam (FIB) box used for the preparation of the cross section of the interface Pb/d-$Al_{13}Co_4$ thin film.

unit. Both surface composition analysis and secondary electron (SE) imaging of the particles were undertaken within the SAM. The base pressure in the SAM chamber was 1×10^{-8} Pa. The surface of the Pb film was first cleaned by ion bombardment, to remove surface contamination gathered during sample transfer. Then the sample was gradually heated, with periodic interruptions during which it was lightly sputtered so as to remove any impurities that may have segregated to the surface. The temperature was given by a thermocouple in contact with the substrate and calibration of the thermocouple was beforehand checked with the melting temperature of lead. The cleaning process was monitored by Auger electron spectroscopy (AES).

To optimize the wetting measurements and allow measurements of contact angles, the droplets were 'frozen' by decreasing the temperature below the melting point of Pb. Then the sample was transferred to a field emission gun scanning electron microscope (SEM) where images of the droplets were obtained with a high resolution (magnification from 4×10^3 to 10^5). Since there was no significant change of the shape of the droplets after solidification, the measured contact angles were taken as those of the frozen-in Pb droplets.

Finally, in order to carefully look at the interface between the metal and the surface of the thin film, and in particular to analyse whether diffusion phenomena between the film and the substrate had occurred, cross section transmission electron microscopy (XTEM) observations were conducted on a Jeol JEM 2010F instrument. The cross sections were prepared with the help of a focused ion beam (FIB) Philips 200 TEM. Figure 1 displays the FIB box which was used for the thinning of the cross section in order to characterize the interface.

5. Results

The sample was heated above the melting point of Pb (600 K) and once this temperature achieved, the lead film dewetted the substrate by forming droplets. The temperature was maintained about 20 K above 600 K during 2 h. During this isothermal stage, no change in the droplets form occurred. The Pb droplets always displayed contact angles lower than 90°.
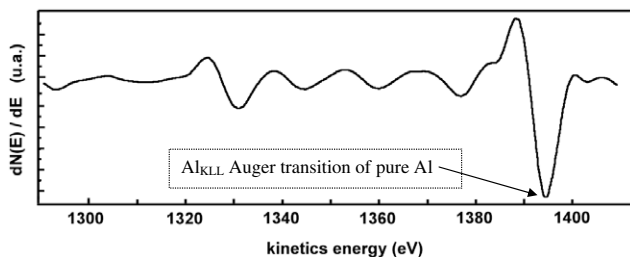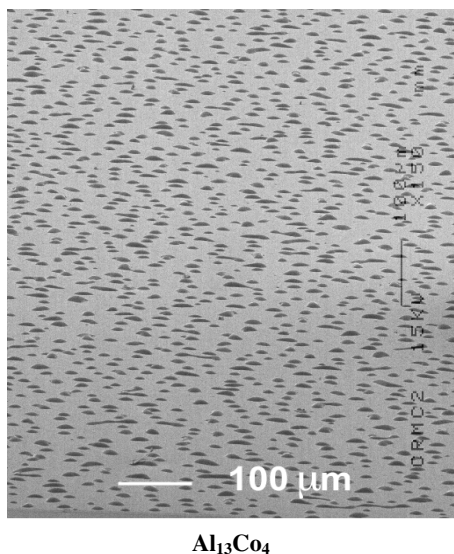
Figure 2. Auger spectrum in the derivative mode of the d-Al$_{13}$Co$_4$ substrate between Pb droplets taken after fragmentation (melting) of the Pb layer. It displays the KLL Auger transition of Al only.
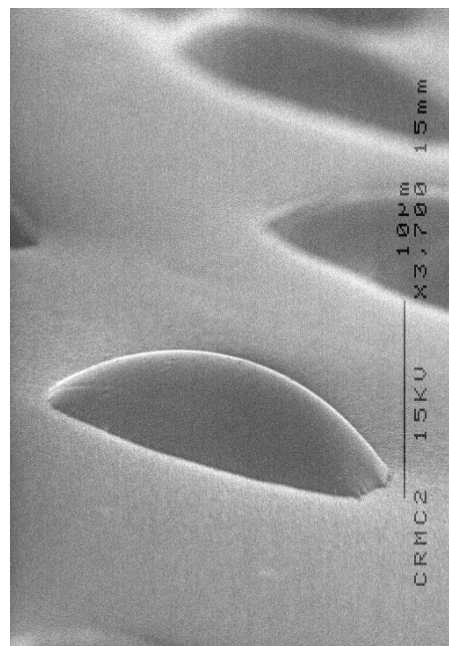

Figure 3. Low magnification SEM images (150×) of the distribution of the Pb droplets lying on the d-Al$_{13}$Co$_4$ thin film after solidification.

Figure 4. High magnification SEM images (3700×) of Pb droplets on the d-Al$_{13}$Co$_4$ thin film after solidification. Several such images were used to measure the contact angles.
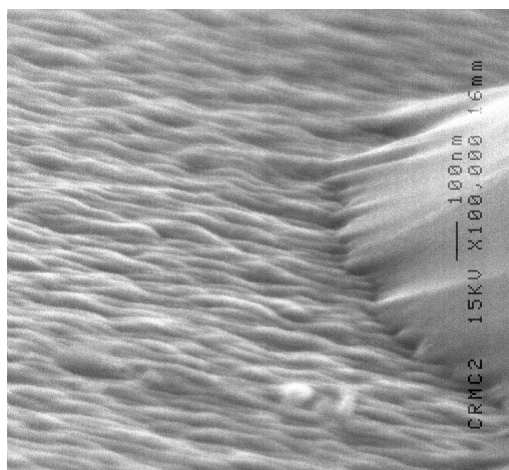

Figure 5. Ultra high magnification SEM images (10^5×) of the pseudopods at the edge of a Pb droplet.

The surface chemistry of the films in the region left uncovered between the droplets was examined by AES. No carbon was detected but oxygen is present in small quantities at the surface of the d-Al$_{13}$Co$_4$ films although not on the surface of the lead drop. Figure 2 displays an Auger spectrum at high energy, in the derivative mode, where the Auger transition of aluminium appears as metallic. Indeed, it is important to emphasize that the Auger transition characteristic of an aluminium oxide is different from that of metallic aluminium [36]. Thus we conclude that the oxygen detected at the surface between the Pb droplets is present as adsorbed species at the surface of the d-Al$_{13}$Co$_4$ compounds.

Figure 3 is a general view of the distribution of the Pb droplets observed by SEM at low magnification. It displays Pb droplets uniformly distributed on the surface of the thin film. The contact circles have diameters of several micrometres. Details of typical Pb droplets on which the contact angles are measured can be seen on figure 4. The contact angles, averaged over several droplets, are 49° ± 7°. At higher magnification, the SEM images (figure 5) allow the observation of the length scale of the roughness of the film which can be estimated to few tenths of nanometres. At this scale, we can see that pseudopods on the drops are developing along the ridges.

However, it was interesting to proceed with further investigations in order to answer the following questions: do grain boundaries play a role for example in pinning the liquid drop? Or does surface or volume diffusion of lead occur in the film during the experiment ? For that purpose, cross sections of the interface between a lead droplet and the surface of the film were prepared and investigated by XTEM; successively from the bottom up, the Si wafer, the SiO$_2$ layer, the nanometric film (after heat treatment) and the drop of lead recovered by a very thin Pt layer (deposited during the preparation of the cross section) can be seen in figure 6. At higher magnification, figure 7 displays a TEM cross section of the Al/Co multilayers
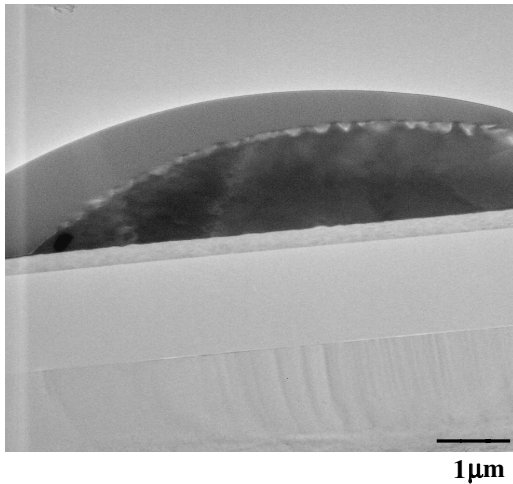
Figure 6. Low magnification transmission electron microscopy cross section showing the successive layers: oxidized Si wafer, d-Al$_{13}$Co$_4$ thin film and the lead droplet covered by Pt thin layer.

150 nm

Figure 7. High magnification transmission electron microscopy cross section showing the interface of the lead droplet with the d-Al$_{13}$Co$_4$ thin film.

heat treated up to 700 K before deposition of a Pb layer showing the trace of the initial stacking of the layers.

Further characterization carried out by AES shows the absence of a continuous film of lead between the droplets at the extreme surface of the film. Note also that rarely we observe some 'streaks' of lead in-between the droplets.

Besides, the contact angle directly measured on the cross section is in agreement with the averaged value obtained from the SEM observations.

6. Discussion

The contact angle of a liquid on a homogeneous surface is given by the Young equation:

$$\cos\theta = \frac{\gamma_{SV} - \gamma_{SL}}{\gamma_{LV}} \qquad (1)$$

where the γ_{ij} are the interface energy of the three interfaces (L = liquid, S = solid and V = vapour).

It should be emphasized that once the contact angle and the surface energy (surface tension) of the liquid are known, equations (1) only gives the difference between the solid/liquid and solid/vapour energies, but not the absolute value of the surface energy of the compound.

To our knowledge there are only estimates but no data on the surface energies of intermetallic compounds. However, we can compare the wetting behaviour of Pb (20 K above its melting point) on the d-Al$_{13}$Co$_4$ compound with the behaviour of Pb on Al$_2$O$_3$, on pure Al and Co, and on the cubic crystalline compound AlCo.

The contact angles of Pb on alumina single crystal and on thick native oxide of aluminium have been reported to be 127° ± 3° and 130° ± 5°, respectively [37]. They are much larger than 90°. Comparison of these contact angles with those measured for the d-Al$_{13}$Co$_4$ compound shows clearly that the Pb droplets do not lie on aluminium oxide, as already suggested by the Auger spectrum of figure 2. On the other
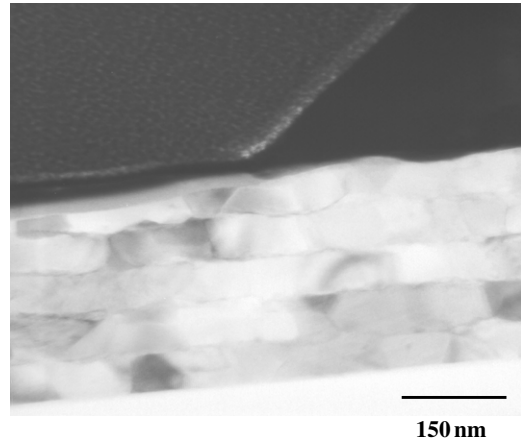
hand, contact angles of Pb on polycrystalline film of Al and on aluminium single crystal are much smaller and close to 30° ± 5° [37, 38]. On polycrystalline films of Co, the contact angle of Pb has been reported to be 50° ± 6° [39], similar to that on d-Al$_{13}$Co$_4$. Moreover, under the same experimental conditions we have shown that this angle is equal to 42° ± 7° in the case of cubic AlCo compound, one of the stable compounds in the phase diagram, with a different crystal structure than the CsCl type [15]. This has been interpreted as the fact that in these conditions 'the quasicrystallinity' is not the parameter which influences significantly the wetting mechanism.

It is interesting to note that, as shown in a study on rapid solidification [40], the melting temperature of lead particles embedded in an AlCuFe icosahedral matrix is lowered than when embedded in a crystalline matrix. This behaviour, linked to the surface energy of the Pb drop embedded in the matrix, shows that this latter differs from the crystalline matrix to the QC one (for more recent review, see Singh and Tsai in this current issue [41]).

The experiment described here is one of dewetting. Upon melting, the slab of Pb retracts into droplets. The equilibrium contact angle is well below 90°. From the observation of figure 5, we can infer that the surface of the films presents some granularity. We shall see that this indicates partial wetting of the Al–Co compounds either due to the granularity of their surface or because full thermodynamic equilibrium was not reached when liquid Pb was frozen-in by cooling under its melting temperature.

Let us return to the derivation of the Young equation (1), and to the physical meaning of the tensions γ. Quoting Bouasse[5] [42], 'surface tension of an interface between two materials is only the expression, independent of any mechanism, of the existence of a surface potential energy proportional to the contact area'. Thus, a solid, partially wet, has a surface energy $\gamma_{SL}a_L + \gamma_{SV}a_V$, where $a_{L,V}$ are the area of contact of the solid with the liquid and the vapour,

---

[5] Here, the contact angle θ is defined so that it is zero for complete wetting. The complementary angle $\alpha = \pi - \theta$ (=180° for complete wetting) is used by Bouasse.

respectively. On a macroscopic scale, the surface of the solid is planar, and the surface of the liquid drops is smooth. An infinitesimal element ds of the contact line is subjected to the normal tensions γ_{SL}ds, γ_{SV}ds on the plane, and γ_{LV}ds at an angle θ from the plane. The condition for equilibrium of the contact line in the plane yields the Young equation (1) for the contact angle of the interface LV. Note that, at equilibrium, the tendency for the solid to be wet (covered by the liquid) is proportional to $\gamma_{SV} - \gamma_{SL}$ (the contact line is pulled towards the vapour side), and the tendency to dewet is proportional to $\gamma_{SL} - \gamma_{SV}$, so that non-wetting occurs if $\gamma_{SL} > \gamma_{SV}$ (and the equilibrium angle θ is obtuse). Since no Pb is detected between droplets, we assumed in the following that this is the equilibrium situation, which was actually reached during our experiment before the (equilibrium) shape of the droplet was reached upon cooling. For liquid Pb on Al–Co, $\gamma_{SL} + \gamma_{LV} > \gamma_{SV} > \gamma_{SL}$. The first inequality indicates that a molten slab of Pb retracts into droplets (with a finite equilibrium contact angle). The second shows that the system does not completely dewet, and that the equilibrium contact angle remains <90°.

Consider now partial (de)wetting: the solid surface is microscopically rough, and the liquid is in contact only with the top of the ridges of the solid [43], making bridges in-between (see figure 2 of [44], or de Gennes review [45]). Under the bridges, the solid is in contact with the vapour. Thus, the normal tension on the liquid side γ_{SL}ds is replaced by $[\rho\gamma_{SL} + (1 - \rho)\gamma_{SV}]ds$, where $0 \leqslant \rho = a_L/a_V \leqslant 1$ is the proportion of the solid wet (on the liquid side of the contact line). The equilibrium equation for the element ds of the contact line in a rough, partially wet solid is

$$\gamma_{SV} - [\rho\gamma_{SL} + (1 - \rho)\gamma_{SV}] - \gamma_{LV}\cos\theta$$
$$= \rho\gamma_{SV} - \rho\gamma_{SL} - \gamma_{LV}\cos\theta = 0.$$

Thus, for liquid Pb on a *rough* (at a scale much smaller than the size of the individual droplets) d-Al$_{13}$Co$_4$ compound, the cosinus of the contact angle is in the range, $0 < \cos\theta = \rho[\gamma_{SV} - \gamma_{SL}]/\gamma_{LV} < 1$. For $\rho = 1$ (smooth solid surface) one recovers the standard Young equation. For $\rho \approx 0$, the contact angle is maximum, $\theta \approx 90°$. On a rough material involving partial wetting, the contact angle θ is large, but never obtuse.

Now, if the element ds of the contact line lies on the ridge, the proportion of the solid wet (perpendicular to ds) is $\rho \approx 0$, and $\theta = 90°$. Indeed, the drops of liquid on a rough solid with parallel stripes are semicylindrical. If the ridge cuts perpendicularly across the contact line, one has $\rho = 1$ and a low value of θ. This can be seen in the pseudopods on the drops of figure 5, that correspond to liquid lagging behind in the retracting drop, because it wets the ridges perpendicular to the circular contact line. For an arbitrary orientation λ of the ridge with ds, $\rho = \sin\lambda$ with probability (flux) of a ridge cutting across ds given by d$P = (1/2)\sin\lambda$ dλ, so that, on average over the circular rim of the drop, $\langle\rho\rangle = \langle\sin\lambda\rangle = \pi/4 = 0.79$ and $\cos\theta = 0.79[\gamma_{SV} - \gamma_{SL}]/\gamma_{LV}$, independent of the crystalline or quasicrystalline structure of the material, as long as it is rough.

Our measurements of $\theta \approx 45°$ (value averaged on the two d-Al$_{13}$Co$_4$ and cubic AlCo films) yield a relation between the surface tensions of liquid Pb on a smooth Al–Co compound,

$[\gamma_{SV} - \gamma_{SL}]/\gamma_{LV} = (1/\sqrt{2})/\langle\rho\rangle = 2\sqrt{}/\pi = 0.9$. Then we can predict, from the standard Young relation, the contact angle of the same material Pb on a smooth Al–Co substrate $\theta = 26°$ which is accordingly much smaller than the measured contact angle of 45° on a rough substrate.

In conclusion, the contact angle of a drop of a low melting point metal, Pb, on a surface of a quasicrystalline decagonal compound d-Al$_{13}$Co$_4$ has been recently measured to be 49° ± 7° [15]. A peculiar experimental method has been developed to prevent the formation of an aluminium oxide layer on the surface of the film before the measurements. In this paper, a careful study of the interface from the micrometre to the nanometre scale is reported. Further characterization carried out by AES shows the absence of a continuous film of lead between the droplets at the extreme surface of the film. If we assume a certain rugosity of the surface of the film, confirmed by our SEM observations, the existence of partial dewetting due to the fact that the surface is not smooth, leads to a smaller value of the contact angle. The comparison of the wetting behaviour of a cubic crystalline compound of the same Al/Co system does not show a significant influence of the structure. It is interesting to note that both compounds are aluminium-rich, but they are not wetted by Pb like a simple metal such as aluminium and that their wetting behaviour is closer to that on a surface of a metal of high melting point.

The main interest of this experiment is that, for the first time, wetting properties have been measured without any oxygen contamination.

The effects of the structure of the Al–Co compound and of its surface can then be assessed: the latter (rough or smooth) matters very much while the former, whether crystalline or quasicrystalline, only slightly. This is not so when wetting experiments are conducted against polar liquids like water (see Dubois *et al*, elsewhere in this issue [46]).

Acknowledgments

References

[1] Levine D and Steinhardt P J 1986 *Phys. Rev.* B **34** 596
[2] Shechtman D, Blech I, Gratias D and Cahn J-W 1984 *Phys. Rev. Lett.* **53** 1951
[3] Fischer I R, Islam Z, Panchula A F, Cheon K O, Kramer M J, Canfield P C and Goldman A I 1998 *Phil. Mag.* B **77** 1601
[4] Delahaye J, Brison J P and Berger C 1998 *Phys. Rev. Lett.* **81** 4204
[5] Stadnik Z M 1999 *Physical Properties of Quasicrystals* (Berlin: Springer)

[6] Kang S and Dubois J M 1992 *Phil. Mag.* A **66** 151
[7] Dubois J M, Kang S S and von Stebut J 1991 *J. Mater. Sci. Lett.* **10** 537
[8] Dubois J M 1997 *New Horizons in Quasicrystals: Research and Applications* ed A I Goldman, D J Sordelet, P A Thiel and J M Dubois (Singapore: World Scientific) p 208
[9] Dubois J M 2005 *Useful Quasicrystals* (Singapore: World Scientific)
[10] Gavatz M, Rouxel D, Claudel D, Pigeat P, Weber B and Dubois J M 1998 *Proc. 6th Int. Conf. on Quasicrystals* ed S Takeuchi and T Fujiwara (Singapore: World Scientific) p 765
[11] Rouxel D and Pigeat P 2006 *Prog. Surf. Sci.* **81** 488
[12] Belin-Ferré E 2002 *J. Phys.: Condens. Matter* **14** 789
[13] Thiel P A 2004 *Prog. Surf. Sci.* **75** 69
[14] Chevrier J 2000 *Quasicrystals: Current Topics* ed E Belin-Ferre, C Berger, M Quiquandon and A Sadoc (Singapore: World Scientific) p 303
[15] Bergman C, Girardeaux C, Perrin-Pellegrino C, Gas P, Chatain D, Dubois J M and Rivier N 2006 *Phil. Mag.* **86** 849
[16] Bauer E 1958 *Z. Kristallogr.* **110** 372
[17] Bauer E and Poppa H 1972 *Thin Solid Film* **12** 167
[18] Frank C and van der Merwe J H 1949 *Proc. R. Soc. Lond.* A **198** 205
[19] Stranski N and Von Krastanov L 1939 *Akad. Wiss. Lit. Mainz Mat.-Natur. Kl.* IIb **146** 797
[20] Volmer M and Weber A 1926 *Z. Phys. Chem.* **119** 277
[21] Shimoda M, Sato T J, Tsai A P and Guo J Q 2002 *J. Alloys Compounds* **342** 441
[22] Fournée V, Cai T C, Ross A R, Lograsso T A, Evans J W and Thiel P A 2003 *Phys. Rev.* B **67** 033406
[23] Wearing L H, Smerdon J A, Leung L, Lograsso T A, Ross A R and McGrath R 2007 *Surf. Sci.* **601** 3450
[24] Leung L, Ledieu J, Unsworth P, Lograsso T A, Ross A R and McGrath R 2006 *Surf. Sci.* **600** 4752
[25] Sharma H R, Shimoda M and Tsai A P 2007 *Adv. Phys.* **56** 403
[26] Philibert J 1991 *Appl. Surf. Sci.* **53** 74
[27] Bogatyrev A O, Hodaj F and Gusak A M 2001–2002 *Bull. Cherkasy State Univ. Phys.* **37/38** 89
[28] Yeh X L, Samwer K and Johnson W L 1983 *Appl. Phys. Lett.* **42** 242
[29] Grushko B, Wittenberg R, Bickman K and Freiburg C 1996 *J. Alloys Compounds* **233** 279
[30] Ma X L and Kuo K H 1992 *Metall. Trans.* A **23** 1121
[31] Ma X L and Kuo K H 1994 *Metall. Trans.* A **25** 47
[32] Gödecke T and Ellner M 1996 *Z. Metallk.* **87** 854
[33] Grushko B, Freiburg C, Bickman K and Wittenberg R 1997 *Z. Metallk.* **88** 5
[34] Emeric E, Bergman C, Clugnet G, Gas P and Audier M 1998 *Phil. Mag. Lett.* **78** 77
[35] Wang Z, Wynblatt P and Chatain D 1999 *Interface Sci.* **7** 173
[36] Davis L E, MacDonald N C, Palmberg P W, Riach G E and Weber R E 1976 *Handbook of Auger Electron Spectroscopy* 2nd edn (Minnesota: Physics Electronics Industries) pp 43–7
[37] Lesueur C, Chatain D, Bergman C, Gas P and Baqué F 2002 *J. Physique* IV **12** 155
[38] Shi Z, Lowekamp J and Wynblatt P 2002 *Metall. Mater. Trans.* A **33** 1003
[39] Chatain D 2008 at press
[40] Singh A and Tsai A P 1998 *Acta Mater.* **46** 4641
[41] Singh A and Tsai A P 2008 *J. Phys.: Condens. Matter* **20** 314002
[42] Bouasse H 1924 *Capillarité* (Paris: Delagrave)
[43] Menchaca Rocha A 1992 *J. Colloid. Interface. Sci.* **149** 472
[44] Rivier N 1997 *New Horizons in Quasicrystals: Research and Applications* ed A I Goldman, D J Sordelet, P A Thiel and J M Dubois (Singapore: World Scientific) p 188
[45] de Gennes P G 1985 *Rev. Mod. Phys.* **57** 827
[46] Dubois J M, Fournée V, Thiel P A and Belin-Ferré E 2008 *J. Phys.: Condens. Matter* **20** 314011